Title
Noggin is required for first pharyngeal arch differentiation in the frog Xenopus tropicalis

Journal
Developmental Biology, 426(2)

ISSN
0012-1606

Authors
Young, John J
Kjolby, Rachel AS
Wu, Gloria
et al.

Publication Date
2017-06-01

DOI
10.1016/j.ydbio.2016.06.034

Peer reviewed

HHS Public Access

Author manuscript

Dev Biol. Author manuscript; available in PMC 2018 June 15.

Published in final edited form as:

Dev Biol. 2017 June 15; 426(2): 245–254. doi:10.1016/j.ydbio.2016.06.034.

Noggin is required for first pharyngeal arch differentiation in the frog *Xenopus tropicalis*

John J. Young[1,2], **Rachel A.S. Kjolby**[1], **Gloria Wu**[1,3], **Daniel Wong**[1], **Shu-wei Hsu**[1,4], and **Richard M. Harland**[1]

[1]Department of Molecular Cell Biology, University of California, Berkeley, Berkeley CA 94720

Abstract

The dorsal ventral axis of vertebrates requires high BMP activity for ventral development and inhibition of BMP activity for dorsal development. Presumptive dorsal regions of the embryo are protected from the ventralizing activity of BMPs by the secretion of BMP antagonists from the mesoderm. Noggin, one such antagonist, binds BMP ligands and prevents them from binding their receptors, however, a unique role for Noggin in amphibian development has remained unclear. Previously, we used zinc-finger nucleases to mutagenize the *noggin* locus in *Xenopus tropicalis*. Here, we report on the phenotype of *noggin* mutant frogs as a result of breeding null mutations to homozygosity. Early homozygous *noggin* mutant embryos are indistinguishable from wildtype siblings, with normal neural induction and neural tube closure. However, in late tadpole stages mutants present severe ventral craniofacial defects, notably a fusion of Meckel's cartilage to the palatoquadrate cartilage. Consistent with a *noggin* loss-of-function, mutants show expansions of BMP target gene expression and the mutant phenotype can be rescued with transient BMP inhibition. These results demonstrate that in amphibians, Noggin is dispensable for early embryonic patterning but is critical for cranial skeletogenesis.

Introduction

Transplantation of Spemann's organizer from a gastrulating amphibian embryo to the ventral side of a host induces an ectopic axis with dorsal derivatives such as neural tissue and skeletal muscle. This second axis is the result of an induction by the grafted cells as lineage tracing shows that only the notochord and head mesoderm are derived from the ectopic tissue. This activity is mediated by organizer specific genes that encode secreted proteins (Smith and Harland, 1992; Hemmati-Brivanlou et al., 1994; Sasai et al., 1994; Bouwmeester et al., 1996; Glinka et al., 1998; Pera and De Robertis, 2000). Noggin was among the first molecules to be discovered for their ability to mimic organizer activity and dorsalize

Correspondence to: Richard M. Harland.

[2]Present Address: Department of Genetics, Harvard Medical School, Boston MA 02115

[3]Present Address: Keck School of Medicine, University of Southern California, Los Angeles, CA 90033

[4]Present Address: College of Medicine, University of Central Florida, Orlando FL 32816

surrounding tissue (Smith et al., 1993). These molecules act to antagonize signaling pathways that pattern the axes of the embryo (Zimmerman et al., 1996; Piccolo et al., 1996; Glinka et al., 1998; Niehrs, 2004).

During gastrulation, graded Bone Morphogenetic Protein (BMP) signaling induces ventral fates at high doses, and dorsal fates at low levels. Initially BMP signaling is pervasive but is locally blocked by secretion of BMP antagonists from the dorsal mesoderm, where it protects the surrounding tissue from ventralizing BMP signals. Knockdown or depletion of these antagonists results in a loss of all dorsal structures and the formation of a "belly piece" (Khokha et al., 2005). In Xenopus, Noggin, Chordin, Follistatin, Nodal3 and Cerberus all cooperate to block BMP signaling. Individual or pairwise knockdowns of these three proteins result in no or mild phenotypes (Oelgeschläger et al., 2003, Khokha et al., 2005). For *noggin* this was surprising, since mice lacking the *Noggin* locus have severe neural tube closure and skeletal defects (McMahon et al., 1998). While different species often require similar genes to different extents, this raises the question of whether Noggin is completely dispensable in amphibian development or whether morpholino knockdown is insufficient to reveal the true loss-of-function phenotype.

Sequencing the genome of *Xenopus tropicalis* (Hellsten et al., 2010) and subsequent genomic analysis of *X. laevis* (Session et al. 2016) expands the potential of genetic manipulation in these models using multiple approaches. The last decade has been witness to a revolution in genome editing techniques being applied to cultured cells or developing organisms (Urnov et al., 2010). In zebrafish Zinc-finger nucleases were first used to mutate the *no tail/brachyury* locus (Doyon et al., 2008) and then rapidly adapted for use in rats (Geurts et al., 2010) and *Xenopus* (Young et al., 2011). With quick succession, the discovery of transcription activator like (TAL)-Type III Effectors (TALEs) (Boch et al., 2009) and clustered regularly interspaced short palindromic repeats associated Cas9 (CRISPR/Cas9) (Jinek et al., 2012) were adapted to genome editing techniques which allowed for a myriad of targeted mutations to be made in human cells (Mali et al., 2013), mice (Wang et al., 2013), zebrafish (Hwang et al., 2013), and *Xenopus* (Blitz et al., 2013; Nakayama et al., 2013). These technologies have made it possible to compare morpholino knockdown phenotypes with those of targeted mutations. There have been some reported discrepancies between gene-edited mutants and morpholino phenotypes (Kok et al., 2015), however, these may be due to genomic compensation as a result of mutagenesis (Rossi et al., 2015).

In a previous study, we showed that ZFN-induced mutagenesis was effective in producing loss-of-function and presumably null alleles in the *noggin* locus of *X. tropicalis* (Young et al., 2011). No phenotype was observed in the mutant founder animals, though this is not unexpected as they were mosaic and Noggin is a secreted protein. Therefore, any essential role for Noggin in amphibian embryogenesis remained unclear. Here, we describe the phenotype of homozygous *noggin* mutant embryos and show surprisingly that the mutants develop normally until late tadpoles stages when they begin to display malformations in the lower jaw and die shortly after beginning to feed.

Material and Methods

Embryo Collection, microinjection, and drug treatment

Xenopus tropicalis embryos were collected from natural matings and staged according to Nieuwkoop and Faber (Nieuwkoop, 1967). To induce mating, female *Xenopus tropicalis* were injected with a priming dose of 10 units of human chorionic gonadotropin (HCG), followed the next morning by a boosting dose of 200 units HCG (Chorulon) and were paired with a male injected with 100 units HCG the previous night. Animals in amplexus produced embryos over a 6–8 hour period.

Previously described morpholinos against *chordin* and *follistatin* (Khokha et al., 2005) were injected animally at the two-cell stage and embryos were collected for analysis when siblings reached stage 14. The small molecule BMP type I receptor inhibitor LDN-193189 was dissolved in DMSO and used at either 10μM or 15μM in 1/9 Marc's Ringer solution with gentamycin.

Embryo staining and Genotyping

Embryo mRNAs were stained by whole-mount *in situ* hybridization as previously described (Harland, 1991). *In situ* hybridizations on tadpoles for comparison between wild type and mutant embryos were first stained together in the same reaction and then photographed before genotyping. Tadpoles were screened for heterozygous and homozygous mutations by PCR followed by Cel1 assays as previously described (Young et al., 2011; Young and Harland, 2012). Genotyping tadpoles previously processed for *in situ* were not fixed in Bouin's, instead were lysed with proteinase K (Roche) in thermopol buffer (NEB) for 6 hours at 55°C then incubated at 60°C for 12 hours prior to PCR to reverse crosslinking.

Phospho-histone H3 and TUNEL staining

Tadpoles were fixed, dehydrated in methanol, and after rehydration were embedded in OCT (TissueTek) for sectioning. Slides were blocked with 10% donkey serum and stained overnight using anti-phospho-Histone H3 (Millipore) 1:500 at 4°C. Alexa 488 donkey anti-rabbit secondary (Jackson Labs) was used at 1:250 and counterstained with DAPI. TUNEL staining was done on slides using the *in situ* cell death detection kit (Roche) according to manufacturer's protocol and counterstained with DAPI. The colocalization plugin tool for ImageJ was used to quantitate cells positive for either phospho-Histone H3 or TUNEL.

Cartilage staining

Tadpoles were fixed in 4% paraformaldehyde for 2–24 hours at room temperature in 4 mL vials. Paraformaldehyde was decanted and the embryos were suspended in a sterile filtered solution of acid/alcohol (70% ethanol and .37% HCl) containing 0.1% Alcian Blue (Kimmel et al., 1998). Vials were placed on a rotator and gently mixed for 6–12 hours at room temperature when staining of the cartilage elements becomes apparent. When staining was complete, the buffer was discarded and tadpoles were resuspended in the acid/alcohol solution without alcian blue and rotated for 20 minutes at room temperature. This was repeated until the solution no longer had any blue tint. Tadpoles were then rehydrated stepwise into water and then bleached in 1X SSC supplemented with 1.2% hydrogen

peroxide and 5% formamide for 1–2 hours on a white-light table. Vial caps were removed to vent gases. Following bleaching, tadpoles were resuspended in a 2% KOH solution and rotated for 1 hour. Stained tadpoles were cleared by successive 2 hour incubations in 2% KOH with increasing concentration of glycerol. Once cleared, tadpoles were either directly imaged or flat-mounted on a microscope slide by fine dissection and imaged. For histological sections, tadpoles were dehydrated and embedded in paraffin wax. Sections were cut using a Leica RM2165 microtome and attached to slides. Slides were rehydrated and stained with Alcian Blue and Nuclear Fast Red. Following staining, slides were dehydrated and mounted in Permount (Sigma).

Results

In a previous report, we took advantage of newly developed genomic tools along with sequencing data in *Xenopus* and targeted the *noggin* locus for mutation using zinc-finger nucleases, which produced three lines of frogs carrying different mutant alleles (Young et al., 2011). One such allele previously identified has a four-basepair insertion, which results in a premature stop codon after proline 54 referred henceforth as nog^{RMH3}. To further assess whether nog^{RMH3} is a true null allele in the work presented here, heterozygous adults were crossed and the resulting embryos were injected with morpholinos targeting Chordin and Follistatin. Knocking down Noggin, Chordin, and Follistatin in combination results in a loss of dorsal structures and yields embryos without neural or somitic derivatives; in contrast knocking down any two in combination results in a reduction but not a complete loss of these structures (Khokha et al., 2005). Injected embryos were raised to stage 14 and assayed for *sox2* and *myoD* expression. Genotyping embryos at this stage did not provide reliable results so all injected embryos were processed for *in situ* together in the same reaction so that staining could be compared within each treatment. Uninjected embryos expressed *sox2* throughout the neural plate, *myoD* in the underlying mesoderm, and *cytokeratin* in the non-neural ectoderm (Figure 1A,D,G). Chordin and Follistatin morpholino injection resulted in a reduction of both *sox2* and *myoD* and a slight expansion of *cytokeratin* in ~75% of the embryos (Figure 1B,E,H). However, in approximately 25% of injected embryos, predicted to be those homozygous for the nog^{RMH3} allele, there was a complete loss of both *sox2* and *myoD* expression and a complementary expansion of *cytokeratin* throughout the dorsal ectoderm (Figure 1C,E,I). These results, taken with the failure of nog^{RMH3} RNA to induce ectopic axes (Young et al., 2011) suggest that nog^{RMH3} is a functionally null allele.

Previously, to knock down the activity of Chordin, Follistatin and Noggin in *X. tropicalis* embryos, we needed a very high dose of Morpholino Oligonucleotides. While this dose is high, the phenotype was nonetheless rescuable, and physiologically meaningful (Khokha et al., 2005). In this regard it is interesting to compare the effect of knockdown of Chordin and Follistatin in the context of the *noggin* mutant, where even residual expression of myoD and Sox2 is absent. This suggests that the noggin mutant, in the context of Chordin and Follistatin knockdown, is similar but more extreme in phenotype that the noggin MO injection; this experiment therefore supports the specificity of the *noggin* MO, and also supports the idea that the BMP antagonists have biological function even at very small doses.

Noggin-null mice die at birth due to numerous defects including open neural tubes, spinal cord mispatterning, and several skeletal abnormalities including excess cartilage condensation and failure of joint formation (Brunet et al., 1998; McMahon et al., 1998). Conversely, morpholino knockdown of Noggin, or expression of Noggin blocking antibodies in *Xenopus* does not yield a phenotype (Khokha et al., 2005)). This discrepancy may be due to different biology of Noggin function in the two species, incomplete knockdown by the morpholino or because a requirement for Noggin occurs when morpholinos are losing effectiveness. To distinguish between these possibilities, heterozygous adults carrying nog^{RMH3} were crossed and the resulting embryos were cultured and observed for phenotypic abnormalities. Unexpectedly, we did not observe defects in neural tube closure in any of the embryos produced from heterozygous parents (Figure S1A–J). No defects were observed in any embryos until stage 45 where a dorsal-rostral protuberance along with a concave ventrum was noticed in a subset of the clutch (Figure S1K–N); this phenotype becomes more pronounced at stage 46 (Figure 2A–F). Sorting tadpoles based on the presence or absence of this dorsal “horn” resulted in 2533 (75.1%) wild type (WT) and 824 (24.9%) abnormal (Figure S1K–N) (Table 1). Genotyping 10 phenotypically WT and 10 horned tadpoles revealed the horned tadpoles were always homozygous for the *noggin* null allele.

To determine the nature of the horn observed in *noggin* mutants, alcian blue staining was used to visualize the cartilage skeleton of the cranium (McDiarmid and Altig, 1999). Comparison of stained WT and mutant crania revealed deformations of the ventral skeletal elements (Figure 2G,H). Further, mid-sagittal histological sections through the head revealed that the dorsal protrusion is the cartilaginous suprarostral plate made more prominent because of the reduction in the palatoquadrate and Meckel’s cartilage (arrowheads in Figure 2G’,H’). These defects can be seen in flat mounted cartilage preparations between WT (Figure 2I) and mutant (Figure 2J) tadpoles. These preparations showed that mutants had smaller cartilage elements, in-turned ceratohyals, deformed ceratobranchial cartilage, and most notably severely reduced Meckel’s cartilage that is fused to the palatoquadrate (Figure 2J,J’’). Consistent with smaller crania, mutant tadpoles at stage 46 showed a reduced number of cells positive for phospho-histone H3 (Figure S2A,B) and an elevated number of TUNEL positive cells (Figure S2C–E). In contrast, there are no major differences in the super-rostral plate between the WTs and mutants, indicating that the horn observed in the mutants is due to a deformation and loss of ventral structures (i.e. Meckel’s cartilage and ceratohyals) rather than an overgrowth of the super-rostral plate. Mutant tadpoles did not display obvious sensory defects as they responded to gentle tapping on the culture dish. Finally, the mutants began to die off rapidly by two weeks post fertilization (Figure S3), with food in the pharynx but none in the gut.

Because Noggin is a BMP antagonist (Zimmerman et al., 1996), we reasoned that the observed phenotypes of mutant tadpoles are likely due to increased BMP signaling. To test this hypothesis, we use the small molecule BMP inhibitor LDN193189 (Cuny et al., 2008) to attenuate BMP signaling in developing tadpoles. Adults heterozygous for the nog^{RMH3} allele were crossed and the resulting embryos were raised to stage 28 (Nieuwkoop, 1967) when they were divided into three groups. The first were left untreated, the second were treated with 0.1% DMSO, and the third were treated with LDN193189 for 24 hours. Following treatment, the drug (or DMSO) was washed out and all tadpoles were cultured until stage 46.

If the ventral skeletal defects observed in tadpoles homozygous for the *nog*^{RMH3} allele are due to increased BMP signaling, we reasoned that pharmacologically inhibiting BMP would rescue the phenotype. Indeed, untreated tadpoles showed the expected ratio of WT (n=147,75.8%) to mutant (n=45, 23.2%). Similar ratios were obtained for those treated with DMSO; WT (n=142, 75.9%) and mutant (n=40, 21.3%). Genotyping 10 individuals each from WT (Figure 3A,B and Figure 3E,F) and mutant (Figure 3C,D and Figure 3G,H) tadpoles from untreated and DMSO treated groups confirmed that those exhibiting the mutant phenotype were always homozygous for the *nog*^{RMH3} allele. However, treatment with 10uM LDN-193189 resulted in nearly all treated tadpoles presenting a wild type phenotype (n=182, 91.9%) with only 10 (5%) exhibiting a slight mutant phenotype. To confirm that mutant tadpoles were rescued, 56 phenotypically normal tadpoles from the LDN193189 treated cohort were collected randomly and genotyped, revealing 42 to be WT according to genotype (Figure 3I,J) and 14 to be homozygous for the *nog*^{RMH3} allele but with a WT phenotype (Figure 3K,L,). The ability of the small molecule BMP inhibitor to significantly rescue ($p<0.00001$, chi-squared test) the phenotype associated with the *nog*^{RMH3} allele (Figure 3M) at stage 28 strongly suggests that the observed cranial defects are due to increased BMP signaling that occurs during pharyngeal arch patterning.

BMP signaling is instrumental in the dorsal-ventral patterning of the pharyngeal arches, which in turn develop into the cranial skeleton. Previous work in zebrafish has shown that BMP signaling is sufficient to induce ventral arch fates in intermediate and dorsal regions (Alexander et al., 2011; Zuniga et al., 2011). Since Noggin functions as a BMP antagonist and is expressed in ventral regions of the pharyngeal arches, (Fletcher et al., 2004) we examined WT and mutant tadpoles for the expression of BMP-responsive genes that function in pharyngeal arch development. However, since the mutant phenotype does not manifest until after patterning and differentiation of the pharyngeal arches is complete, it was necessary to correlate a molecular phenotype with the genotype of tadpoles. To that end, tadpoles from stages 33 and 39 were collected for *in situ* hybridization, imaged, and then lysed and processed for genotyping. This made it possible for mutant-specific differences in expression patterns to be determined following genotyping.

The expression of both BMP target genes *msx1* (Figure 4A–D) and *msx2* (Figure 4E–H) (Tríbulo et al., 2003, Hollnagel et al., 1999) showed two discrete domains of expression in the first arch of wild type tadpoles (Figure 4A,C,E,G arrows). However, the mutants displayed a continuous expression domain of *msx1* at stage 33 (Figure 4D, arrowhead) and *msx2* at both stage 33 (Figure 4F) and 39 (Figure 4H) in the mutants. The next BMP target examined, *endothelin1* (*edn1*), was expanded dorsally in the posterior arches of the mutants (Figure 4I,J) at stage 33 but by stage 39 no differences were distinguishable between WT and Mutant tadpoles (Figure 4K,L). Next, *dlx1* was examined in WT and mutant Tadpoles. Similar to *msx1/2*, *dlx1* showed two domains of expression in the first arch of WT tadpoles at both stage 33 (Figure 4M, arrows) and stage 39 (Figure 4O) but only a single domain in the mutants at both stages (Figure 4N,P, arrowheads). Taken together, these results suggest show that the first arch is mispatterned in tadpoles homozygous for the *nog*^{RMH3} allele, which is consistent with the observed defects in Meckel's cartilage in the mutants.

In zebrafish, Hand2 is known to repress *bapx1*, which is required for joint formation between Meckel's cartilage and the palatoquadrate (Miller et al., 2003). Given the relationship between Hand2 and *bapx1* expression and the fusion of Meckel's cartilage to the palatoquadrate of the homozygous mutants (Figure 2J,J'), we investigated whether *hand2* and *bapx1* expression was disrupted in the nog^{RMH3} mutants. *hand2* (Howard et al., 2000; Xiong et al., 2009) exhibited a broader expression domain in the mutants at stage 33 (Figure 5A,B) and stage 39 (Figure 5C,D). Unexpectedly, we found that *bapx1* expression is maintained in the homozygous mutants at both stage 33 (Figure 5E,F) and stage 39 (Figure G,H) but the expression domain associated with the mandibular joint appeared to be shifted dorsally. To confirm whether this expression domain is indeed shifted in the mutants, we measured the length between the mandibular arch (MA) expression of *bapx1* to the ventral limit of the eye (Ey) as a function of the overall length from the cement gland (CG) to the otic vesicle (OV). This measurement was chosen so that variation in tadpole sizes could be normalized. These measurements revealed a slight but not significant dorsal shift in the *bapx1* expression domain at stage 33 but a robustly significant shift by stage 39 (Figure 5I). Taken together, the expansion of the BMP target *hand2* along with the shift in *bapx1* expression in the homozygous mutant tadpoles suggest that the fusion of Meckel's cartilage to the palatoquadrate is likely a result from this altered patterning.

Discussion

The BMP antagonist Noggin was the first organizer transcript to be discovered that encodes a secreted protein and has since been found to be an important in several developmental contexts. Heterozygous mutations in human *NOGGIN* result in joint fusions in the phalanges associated with proximal symphalangism (SYM1), multiple synostoses syndrome (Gong et al., 1999), brachydactyly (Lehmann et al., 2007), and stapes ankylosis where the inner ear bones are fused congenitally (Brown et al., 2002). However, since its first discovery in amphibians, a role for *noggin* in frog development has remained elusive. The work described above used lines of *Xenopus tropicalis* with ZFN-induced mutations in the *noggin* locus, which revealed it to be required for craniofacial skeletogenesis via BMP signaling inhibition. The work presented here confirms a role for Noggin in amphibian development and is consistent with previous reports of Noggin function in *Xenopus*. Morpholino studies targeting *noggin* resulted in no observable phenotype, which was interpreted as it having a redundant role with other BMP antagonists in neural induction. Accordingly, we observed no phenotypes in *noggin* mutants during early embryogenesis. As shown above, *noggin* mutants do not present a phenotype until feeding stages, which would be unlikely to be revealed by knockdown strategies due to the transient effectiveness of morpholinos (Nutt et al., 2001).

Breeding the induced *noggin* mutant alleles to homozygosity revealed that Noggin functions in the development and differentiation of the pharyngeal arches. Specifically, Noggin appears to be required to restrict expression of the BMP target gene *hand2*. Mutant tadpoles express *hand2* in a broader domain, including the mandibular arch which gives rise to Meckel's cartilage. This provides a potential mechanism to explain the loss of joint formation between Meckel's cartilage and the palatoquadrate observed in mutant tadpoles. Hand2 represses the homeobox gene *bapx1* (Miller et al., 2003). It is plausible that in *noggin*

mutant tadpoles, the increase in BMP signaling due to a loss of Noggin, results in the expansion of Hand2 and a concomitant shift in *bapx1* expression, causing the fusion of Meckel's cartilage to the palatoquadrate (Figure 2H,H'). This may also explain the lethality in mutants two weeks post fertilization. Meckel's cartilage forms the mandible and the severe reduction/loss of this structure in *noggin* mutants impedes the tadpole's ability to feed effectively and likely results in starvation. This is consistent with the inverse sigmoidal survival curve observed in the mutants (Figure S3).

The fusion of skeletal elements in the cranial skeleton is a common phenotype observed in vertebrates with altered BMP signaling during development. Mice that express a constitutively active *BMPr1a* allele in their cranial neural crest cells have craniosynostosis, wherein the sutures of the skull fuse prematurely, which can be rescued by treatment with the BMP inhibitor LDN-193189 (Komatsu et al., 2013). In mutant tadpoles, we observed a fusion at the mandibular joint yet there were several other abnormalities associated with the noggin mutant phenotype. Principal among these was the obvious "horn" (Fig. 2D–F) that is first observed at stage 44. One explanation for this is that the ventral defects due to increased BMP signaling result in the rostral plate becoming more prominent. However, though our gene expression analysis did not show any differences in the dorsal cranium between WT and mutant tadpoles, mice with elevated BMP signaling in the nasal cartilage have a similar upturned nasal bone (Hayano et al., 2015). This is due to a Smad1 and 5 dependent upregulation of p53, which results in increased apoptosis and a failure of the nasal septum to fuse with the secondary palate. While our experiments did not reveal a similar mechanism, it remains possible that increased BMP signaling as a result of Noggin loss may have a similar effect in amphibians.

As mentioned above, *Noggin* mutant mice show neural tube closure defects (McMahon et al., 1998). While the skeletal deformities are consistent between mutant frogs and mice, it remains unknown why there are no defects in the neural tube observed in *noggin* mutant *Xenopus* tadpoles. One explanation could be the presence of other BMP antagonists. Chordin and Follistatin are expressed in a similar domain during early embryogenesis of *Xenopus* (Khokha et al., 2005) and could compensate for the loss of *noggin* in neural patterning. Indeed, there is redundancy in the function of these BMP antagonist during neural induction and dorsalization of the mesoderm (Khokha et al., 2005). A second explanation could be that the paralog *noggin2* gene partially compensates for the loss of *noggin* (Fletcher et al., 2004).

The mutation in *noggin* reported here was generated via designer zinc-finger nucleases (Young et al., 2011). In addition to ZFNs, alternative methods for genome editing have been developed such as transcription activator-like effectors (TALEs) fused with FokI nucleases to generate TALEs (Christian et al., 2010; Cermak et al., 2011). and CRISPR/CAS9 methods (Jinek et al., 2012; Hwang et al., 2013). These editing techniques are powerful methods for generating mutations for the loss-of-function studies and have emerged as an alternative to antisense methods. However, recent controversies have erupted over the accuracies associated with each strategy (Kok et al., 2015; Rossi et al., 2015). The work presented here supports the conclusion that morpholino phenotypes are in concordance with mutant phenotypes (Chung et al., 2014; Bhattacharya et al., 2015). It will be interesting to develop

targeted mutagenesis with homologous recombination techniques in order to generate tissue-specific mutants and assay other potential effects, such as those found in the skeleton of mutant mice (Brunet et al., 1998). Finally, this work emphasizes the value of the genomic sequence of *X. tropicalis.* The recent publication of the *X. laevis* genome also presents an opportunity to use these technologies in *X. laevis* to model human genetic disorders (Bhattacharya et al., 2015).

Supplementary Material

Refer to Web version on PubMed Central for supplementary material.

Acknowledgments

We thank Craig Miller for insightful discussions and Jim Evans and Katie Boyle for animal care. This work was supported by NIH grants GM 49346, GM 42341, and NIH DC011901.

References

Alexander C, Zuniga E, Blitz IL, Wada N, Le Pabic P, Javidan Y, Zhang T, Cho KW, Crump JG, Schilling TF. Combinatorial roles for BMPs and Endothelin 1 in patterning the dorsal-ventral axis of the craniofacial skeleton. Development. 2011

Bhattacharya D, Marfo CA, Li D, Lane M, Khokha MK. CRISPR/Cas9: An inexpensive, efficient loss of function tool to screen human disease genes in Xenopus. Dev Biol. 2015; 408:196–204. [PubMed: 26546975]

Blitz IL, Biesinger J, Xie X, Cho KWY. Biallelic genome modification in F(0) Xenopus tropicalis embryos using the CRISPR/Cas system. Genesis. 2013; 51:827–834. [PubMed: 24123579]

Boch J, Scholze H, Schornack S, Landgraf A, Hahn S, Kay S, Lahaye T, Nickstadt A, Bonas U. Breaking the code of DNA binding specificity of TAL-type III effectors. Science. 2009; 326:1509–1512. [PubMed: 19933107]

Bouwmeester T, Kim S, Sasai Y, Lu B, De Robertis EM. Cerberus is a head-inducing secreted factor expressed in the anterior endoderm of Spemann's organizer. Nature. 1996; 382:595–601. [PubMed: 8757128]

Brown DJ, Kim TB, Petty EM, Downs CA, Martin DM, Strouse PJ, Moroi SE, Milunsky JM, Lesperance MM. Autosomal dominant stapes ankylosis with broad thumbs and toes, hyperopia, and skeletal anomalies is caused by heterozygous nonsense and frameshift mutations in NOG, the gene encoding noggin. Am. J. Hum. Genet. 2002; 71:618–624. [PubMed: 12089654]

Brunet LJ, McMahon JA, McMahon AP, Harland RM. Noggin, cartilage morphogenesis, and joint formation in the mammalian skeleton. Science. 1998; 280:1455–1457. [PubMed: 9603738]

Cermak T, Doyle EL, Christian M, Wang L, Zhang Y, Schmidt C, Baller JA, Somia NV, Bogdanove AJ, Voytas DF. Efficient design and assembly of custom TALEN and other TAL effector-based constructs for DNA targeting. Nucleic Acids Res. 2011; 39:e82. [PubMed: 21493687]

Christian M, Cermak T, Doyle EL, Schmidt C, Zhang F, Hummel A, Bogdanove AJ, Voytas DF. Targeting DNA double-strand breaks with TAL effector nucleases. Genetics. 2010; 186:757–761. [PubMed: 20660643]

Chung HA, Medina-Ruiz S, Harland RM. Sp8 regulates inner ear development. Proc Natl Acad Sci USA. 2014; 111:6329–6334. [PubMed: 24722637]

Cuny GD, Yu PB, Laha JK, Xing X, Liu J-F, Lai CS, Deng DY, Sachidanandan C, Bloch KD, Peterson RT. Structure-activity relationship study of bone morphogenetic protein (BMP) signaling inhibitors. Bioorg Med Chem Lett. 2008; 18:4388–4392. [PubMed: 18621530]

Doyon Y, McCammon JM, Miller JC, Faraji F, Ngo C, Katibah GE, Amora R, Hocking TD, Zhang L, Rebar EJ, Gregory PD, Urnov FD, Amacher SL. Heritable targeted gene disruption in zebrafish using designed zinc-finger nucleases. Nat Biotechnol. 2008; 26:702–708. [PubMed: 18500334]

Fletcher RB, Watson AL, Harland RM. Expression of Xenopus tropicalis noggin1 and noggin2 in early development: two noggin genes in a tetrapod. Gene Expr Patterns. 2004; 5:225–230. [PubMed: 15567718]

Geurts AM, Cost GJ, Rémy S, Cui X, Tesson L, Usal C, Ménoret S, Jacob HJ, Anegon I, Buelow R. Generation of gene-specific mutated rats using zinc-finger nucleases. Methods Mol Biol. 2010; 597:211–225. [PubMed: 20013236]

Glinka A, Wu W, Delius H, Monaghan AP, Blumenstock C, Niehrs C. Dickkopf-1 is a member of a new family of secreted proteins and functions in head induction. Nature. 1998; 391:357–362. [PubMed: 9450748]

Gong Y, Krakow D, Marcelino J, Wilkin D, Chitayat D, Babul-Hirji R, Hudgins L, Cremers CW, Cremers FP, Brunner HG, Reinker K, Rimoin DL, Cohn DH, Goodman FR, Reardon W, Patton M, Francomano CA, Warman ML. Heterozygous mutations in the gene encoding noggin affect human joint morphogenesis. Nat Genet. 1999; 21:302–304. [PubMed: 10080184]

Harland RM. In situ hybridization: an improved whole-mount method for Xenopus embryos. Methods Cell Biol. 1991; 36:685–695. [PubMed: 1811161]

Hayano S, Komatsu Y, Pan H, Mishina Y. Augmented BMP signaling in the neural crest inhibits nasal cartilage morphogenesis by inducing p53-mediated apoptosis. Development. 2015; 142:1357–1367. [PubMed: 25742798]

Hellsten U, Harland RM, Gilchrist MJ, Hendrix D, Jurka J, Kapitonov V, Ovcharenko I, Putnam NH, Shu S, Taher L, Blitz IL, Blumberg B, Dichmann DS, Dubchak I, Amaya E, Detter JC, Fletcher R, Gerhard DS, Goodstein D, Graves T, Grigoriev IV, Grimwood J, Kawashima T, Lindquist E, Lucas SM, Mead PE, Mitros T, Ogino H, Ohta Y, Poliakov AV, Pollet N, Robert J, Salamov A, Sater AK, Schmutz J, Terry A, Vize PD, Warren WC, Wells D, Wills A, Wilson RK, Zimmerman LB, Zorn AM, Grainger R, Grammer T, Khokha MK, Richardson PM, Rokhsar DS. The genome of the Western clawed frog Xenopus tropicalis. Science. 2010; 328:633–636. [PubMed: 20431018]

Hemmati-Brivanlou A, Kelly OG, Melton DA. Follistatin, an antagonist of activin, is expressed in the Spemann organizer and displays direct neuralizing activity. Cell. 1994; 77:283–295. [PubMed: 8168135]

Hollnagel A, Oehlmann V, Heymer J, Rüther U, Nordheim A. Id genes are direct targets of bone morphogenetic protein induction in embryonic stem cells. J Biol Chem. 1999; 274:19838–19845. [PubMed: 10391928]

Howard MJ, Stanke M, Schneider C, Wu X, Rohrer H. The transcription factor dHAND is a downstream effector of BMPs in sympathetic neuron specification. Development. 2000; 127:4073–4081. [PubMed: 10952904]

Hwang WY, Fu Y, Reyon D, Maeder ML, Tsai SQ, Sander JD, Peterson RT, Yeh J-RJ, Joung JK. Efficient genome editing in zebrafish using a CRISPR-Cas system. Nat Biotechnol. 2013; 31:227–229. [PubMed: 23360964]

Jinek M, Chylinski K, Fonfara I, Hauer M, Doudna JA, Charpentier E. A programmable dual-RNA-guided DNA endonuclease in adaptive bacterial immunity. Science. 2012; 337:816–821. [PubMed: 22745249]

Khokha MK, Yeh J, Grammer TC, Harland RM. Depletion of three BMP antagonists from Spemann's organizer leads to a catastrophic loss of dorsal structures. Dev Cell. 2005; 8:401–411. [PubMed: 15737935]

Kimmel CB, Miller CT, Kruze G, Ullmann B, BreMiller RA, Larison KD, Snyder HC. The shaping of pharyngeal cartilages during early development of the zebrafish. Dev Biol. 1998; 203:245–263. [PubMed: 9808777]

Kok FO, Shin M, Ni C-W, Gupta A, Grosse AS, van Impel A, Kirchmaier BC, Peterson-Maduro J, Kourkoulis G, Male I, DeSantis DF, Sheppard-Tindell S, Ebarasi L, Betsholtz C, Schulte-Merker S, Wolfe SA, Lawson ND. Reverse genetic screening reveals poor correlation between morpholino-induced and mutant phenotypes in zebrafish. Dev Cell. 2015; 32:97–108. [PubMed: 25533206]

Komatsu Y, Yu PB, Kamiya N, Pan H, Fukuda T, Scott GJ, Ray MK, Yamamura K-I, Mishina Y. Augmentation of Smad-dependent BMP signaling in neural crest cells causes craniosynostosis in mice. Journal of bone and mineral research : the official journal of the American Society for Bone and Mineral Research. 2013; 28:1422–1433.

Lehmann K, Seemann P, Silan F, Goecke TO, Irgang S, Kjaer KW, Kjaergaard S, Mahoney MJ, Morlot S, Reissner C, Kerr B, Wilkie AOM, Mundlos S. A new subtype of brachydactyly type B caused by point mutations in the bone morphogenetic protein antagonist NOGGIN. Am. J. Hum. Genet. 2007; 81:388–396. [PubMed: 17668388]

Mali P, Yang L, Esvelt KM, Aach J, Guell M, DiCarlo JE, Norville JE, Church GM. RNA-guided human genome engineering via Cas9. Science. 2013; 339:823–826. [PubMed: 23287722]

McDiarmid, RW., Altig, R. Tadpoles. University of Chicago Press; 1999.

McMahon JA, Takada S, Zimmerman LB, Fan CM, Harland RM, McMahon AP. Noggin-mediated antagonism of BMP signaling is required for growth and patterning of the neural tube and somite. Genes Dev. 1998; 12:1438–1452. [PubMed: 9585504]

Miller CT, Yelon D, Stainier DYR, Kimmel CB. Two endothelin 1 effectors, hand2 and bapx1, pattern ventral pharyngeal cartilage and the jaw joint. Development. 2003; 130:1353–1365. [PubMed: 12588851]

Nakayama T, Fish MB, Fisher M, Oomen-Hajagos J, Thomsen GH, Grainger RM. Simple and efficient CRISPR/Cas9-mediated targeted mutagenesis in Xenopus tropicalis. Genesis. 2013; 51:835–843. [PubMed: 24123613]

Niehrs CC. Regionally specific induction by the Spemann-Mangold organizer. Nat Rev Genet. 2004; 5:425–434. [PubMed: 15153995]

Nieuwkoop, PD. Normal Table of Xenopus Laevis (Daudin). Garland Pub; 1967.

Nutt SL, Bronchain OJ, Hartley KO, Amaya E. Comparison of morpholino based translational inhibition during the development of Xenopus laevis and Xenopus tropicalis. Genesis. 2001; 30:110–113. [PubMed: 11477685]

Oelgeschläger M, Kuroda H, Reversade B, De Robertis EM. Chordin is required for the Spemann organizer transplantation phenomenon in Xenopus embryos. Dev Cell. 2003; 4:219–230. [PubMed: 12586065]

Pera EM, De Robertis EM. A direct screen for secreted proteins in Xenopus embryos identifies distinct activities for the Wnt antagonists Crescent and Frzb-1. Mech Dev. 2000; 96:183–195. [PubMed: 10960783]

Piccolo S, Sasai Y, Lu B, De Robertis EM. Dorsoventral patterning in Xenopus: inhibition of ventral signals by direct binding of chordin to BMP-4. Cell. 1996; 86:589–598. [PubMed: 8752213]

Rossi A, Kontarakis Z, Gerri C, Nolte H, Hölper S, Krüger M, Stainier DYR. Genetic compensation induced by deleterious mutations but not gene knockdowns. Nature. 2015; 524:230–233. [PubMed: 26168398]

Sasai Y, Lu B, Steinbeisser H, Geissert D, Gont LK, De Robertis EM. Xenopus chordin: a novel dorsalizing factor activated by organizer-specific homeobox genes. Cell. 1994; 79:779–790. [PubMed: 8001117]

Smith WC, Harland RM. Expression cloning of noggin, a new dorsalizing factor localized to the Spemann organizer in Xenopus embryos. Cell. 1992; 70:829–840. [PubMed: 1339313]

Smith WC, Knecht AK, Wu M, Harland RM. Secreted noggin protein mimics the Spemann organizer in dorsalizing Xenopus mesoderm. Nature. 1993; 361:547–549. [PubMed: 8429909]

Tríbulo C, Aybar MJ, Nguyen VH, Mullins MC, Mayor R. Regulation of Msx genes by a Bmp gradient is essential for neural crest specification. Development. 2003; 130:6441–6452. [PubMed: 14627721]

Urnov FD, Rebar EJ, Holmes MC, Zhang HS, Gregory PD. Genome editing with engineered zinc finger nucleases. Nat Rev Genet. 2010; 11:636–646. [PubMed: 20717154]

Wang H, Yang H, Shivalila CS, Dawlaty MM, Cheng AW, Zhang F, Jaenisch R. One-step generation of mice carrying mutations in multiple genes by CRISPR/Cas-mediated genome engineering. Cell. 2013; 153:910–918. [PubMed: 23643243]

Xiong W, He F, Morikawa Y, Yu X, Zhang Z, Lan Y, Jiang R, Cserjesi P, Chen Y. Hand2 is required in the epithelium for palatogenesis in mice. Dev Biol. 2009; 330:131–141. [PubMed: 19341725]

Young JJ, Cherone JM, Doyon Y, Ankoudinova I, Faraji FM, Lee AH, Ngo C, Guschin DY, Paschon DE, Miller JC, Zhang L, Rebar EJ, Gregory PD, Urnov FD, Harland RM, Zeitler B. Efficient targeted gene disruption in the soma and germ line of the frog Xenopus tropicalis using engineered zinc-finger nucleases. Proc Natl Acad Sci USA. 2011; 108:7052–7057. [PubMed: 21471457]

Young JJ, Harland RM. Targeted gene disruption with engineered zinc-finger nucleases (ZFNs). Methods Mol Biol. 2012; 917:129–141. [PubMed: 22956085]

Zimmerman LB, De Jesús-Escobar JM, Harland RM. The Spemann organizer signal noggin binds and inactivates bone morphogenetic protein 4. Cell. 1996; 86:599–606. [PubMed: 8752214]

Zuniga E, Rippen M, Alexander C, Schilling TF, Crump JG. Gremlin 2 regulates distinct roles of BMP and Endothelin 1 signaling in dorsoventral patterning of the facial skeleton. Development. 2011

Highlights

1. Tadpoles homozygous for a null allele in *noggin, nog*^{RMH3}, do not have defects in neural induction but instead have defects in the cranial skeleton caused by deformations in first arch derivatives and die after two weeks post fertilization.
2. These defects are a result of increased BMP signaling and the expression of BMP target genes is altered in homozygous mutants.
3. In Tadpoles homozygous for the *nog*^{RMH3} allele, *hand2* is expanded and *bapx1*, a maker for the Meckels cartilage joint, is significantly shifted dorsally in the mutants which likely results in the first arch defects observed in the mutants.

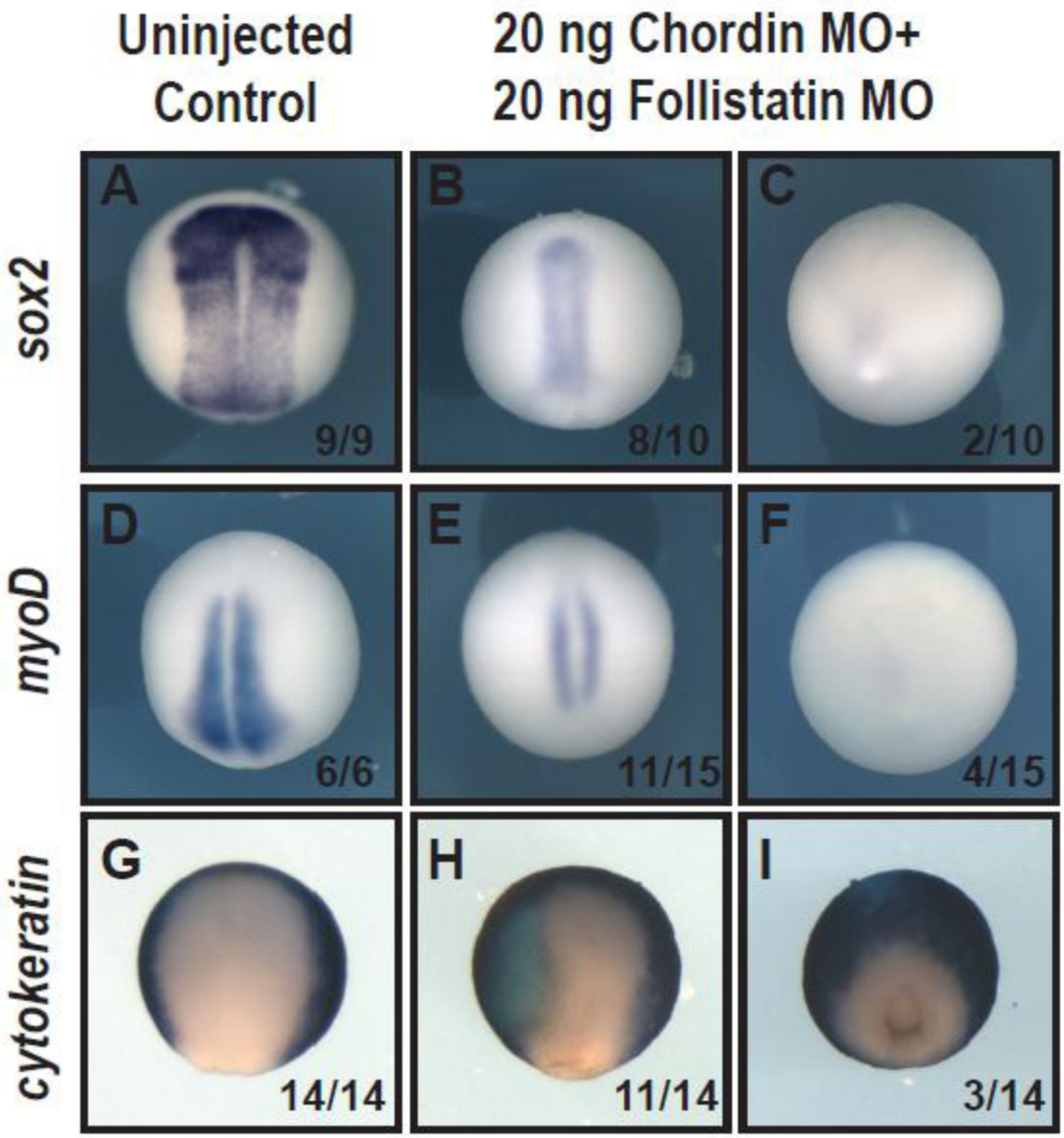

Figure 1. Knockdown of Chordin and Follistatin results in a loss of dorsal structures in a subset of embryos produced by heterozygous *noggin* mutant adults

(A–C) *sox2* expression. (D–F) *myoD* expression. (G–I) *cytokeratin* expression (A,D,G) Uninjected control embryos. (B,C,E,F,H,I) Embryos injected with 20ng Chordin morpholino and 20ng Follistatin morpholino. Dorsal views with anterior towards the top. Though we failed to successfully genotype the stained embryos, the embryos in C, F, and I are predicted to be the *noggin* nulls.

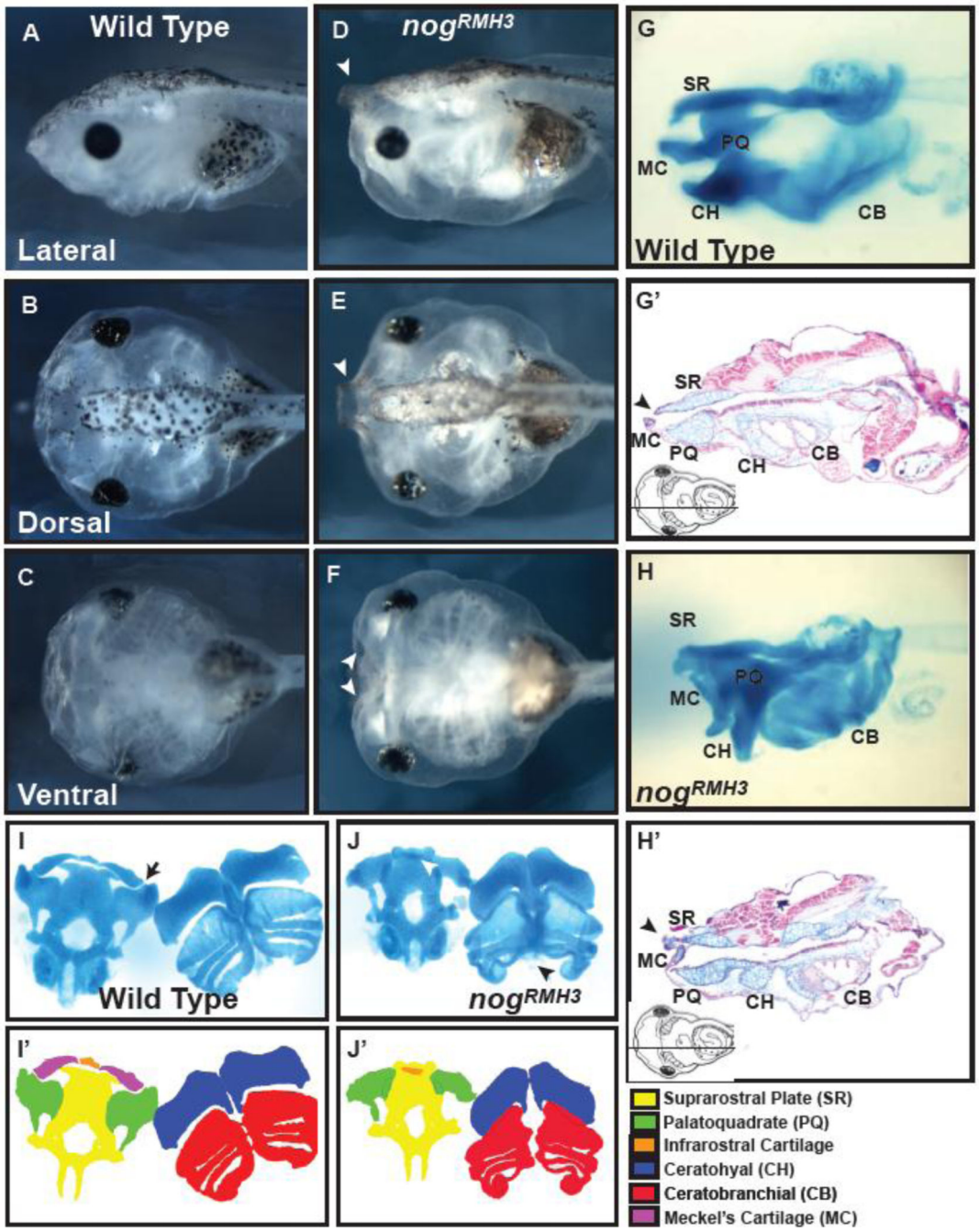

Figure 2. Homozygous *nog*^{RMH3} mutant *Xenopus tropicalis* have severe lower jaw deformities

(A–C) WT stage 46 tadpoles. **(D–F)** Homozygous *nog*^{RMH3} stage 46 tadpoles. Anterior towards the left. (A,D) Lateral views. (B,E) dorsal views. (C,F) Ventral views. **(G–H)** Sagittal views of whole-mount skeletal stains of WT (G) and mutant (H) and 10 micron sagittal sections stained with alcian blue and nuclear fast red of WT (G') and mutant (H') stage 46 skulls. **(I–J)** Flat-mounted cartilage from WT (I) and mutant (J) tadpoles. **(I'–J')** Schematic of skeletal elements in (I–J).

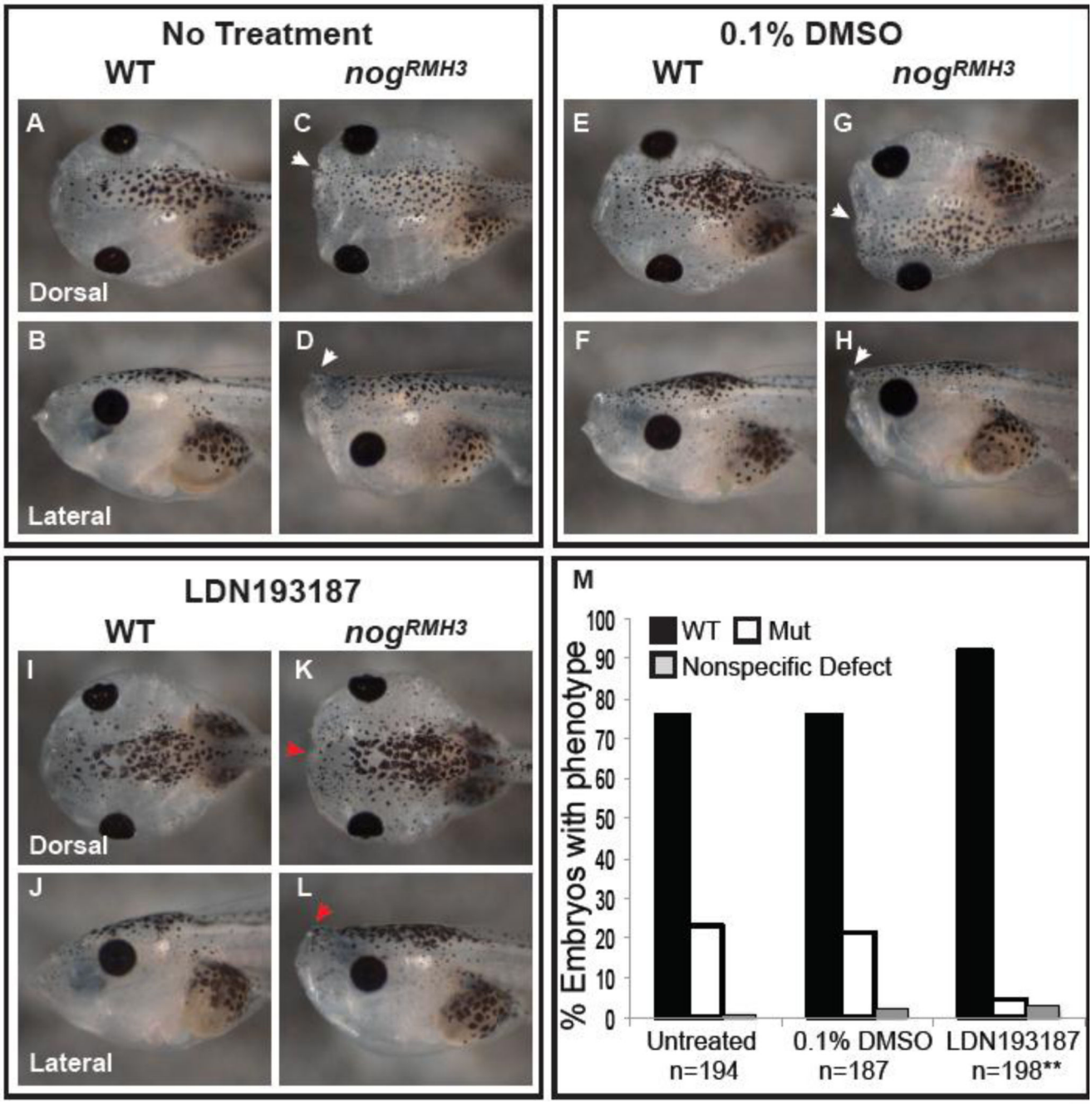

Figure 3. Inhibition of BMP signaling rescues the craniofacial defects observed in the tadpoles homozygous for the *nog*^{RMH3} allele

(A–D) Untreated tadpoles at stage 45 **(E–H)** Tadpoles at stage 45 treated with 0.1% DMSO for 24hrs at stage 28. **(I–L)** Stage 45 tadpoles treated with 10μM LDN-193189 for 24hrs at stage 28. Genotyping showed that the following representative embryos are wild-type (A–B,E–F,I–J), while (C–D,G–H, K–L) are homozygous *nog*^{RMH3} tadpoles. (A,C,E,G,I,K) Dorsal views. (B,D,F,H,J,L) lateral views. White arrowheads show protruding suprarostral plate in the mutants, red arrowheads show rescued structures in mutants following treatment.

(M) Quantification of phenotypes observed following treatments indicated. Black bars show the number of tadpoles with a wildtype phenotype, open bars show the number with the mutant phenotype and gray bars indicate tadpoles with non-specific defects. ** indicates $p<0.0001$.

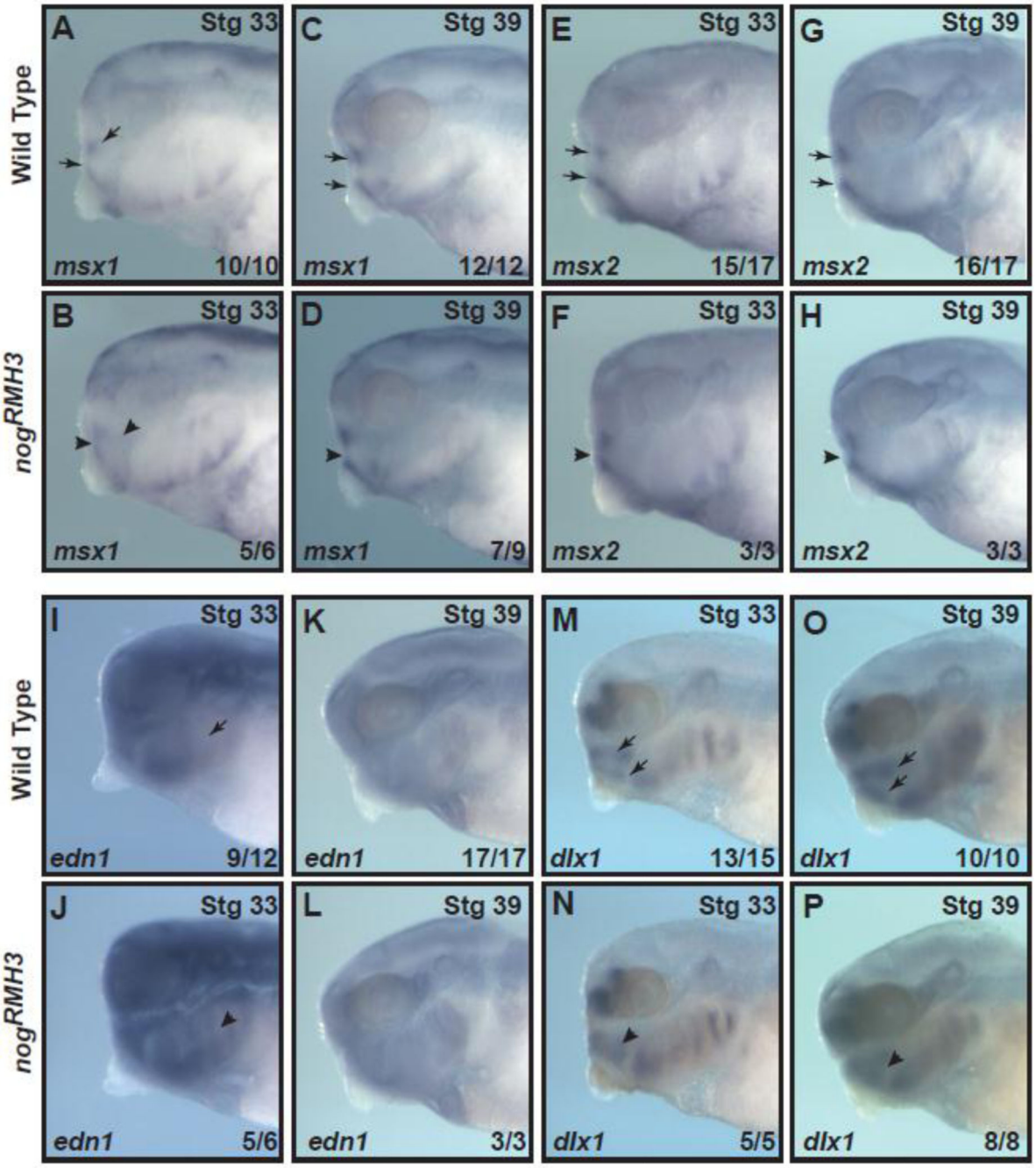

Figure 4. Expression patterns of BMP pathway target genes are affected by the homozygous *nog*^{RMH3} mutanion in a stage specific manner

(A–D) Expression of *msx1* in the head of representative WT (A,C) and homozygous *nog*^{RMH3} (B,D) tadpoles. **(E–H)** Expression of *msx2* in the head of representative WT (E,G) and homozygous *nog*^{RMH3} (F,H) tadpoles. **(I–L)** Expression of *edn1* in the head of representative WT (I,K) and homozygous *nog*^{RMH3} (J,L) tadpoles. **(M–P)** Expression of *dlx1* in the head of representative WT (M,O) and homozygous *nog*^{RMH3} (N,P) tadpoles. (A–B,E–F,I–J,M–N) Stage 33. (C–D,G–H,K–L,O–P) Stage 38. Anterior to the left and dorsal

towards the top. (A,C,E,G,I,K,M,O) Arrows show domains of expression of indicated genes in WT tadpoles. (B,D,F,H,J,L,N,P) Arrowheads show altered expression domains in homozygous *nog*^{RMH3} mutants.

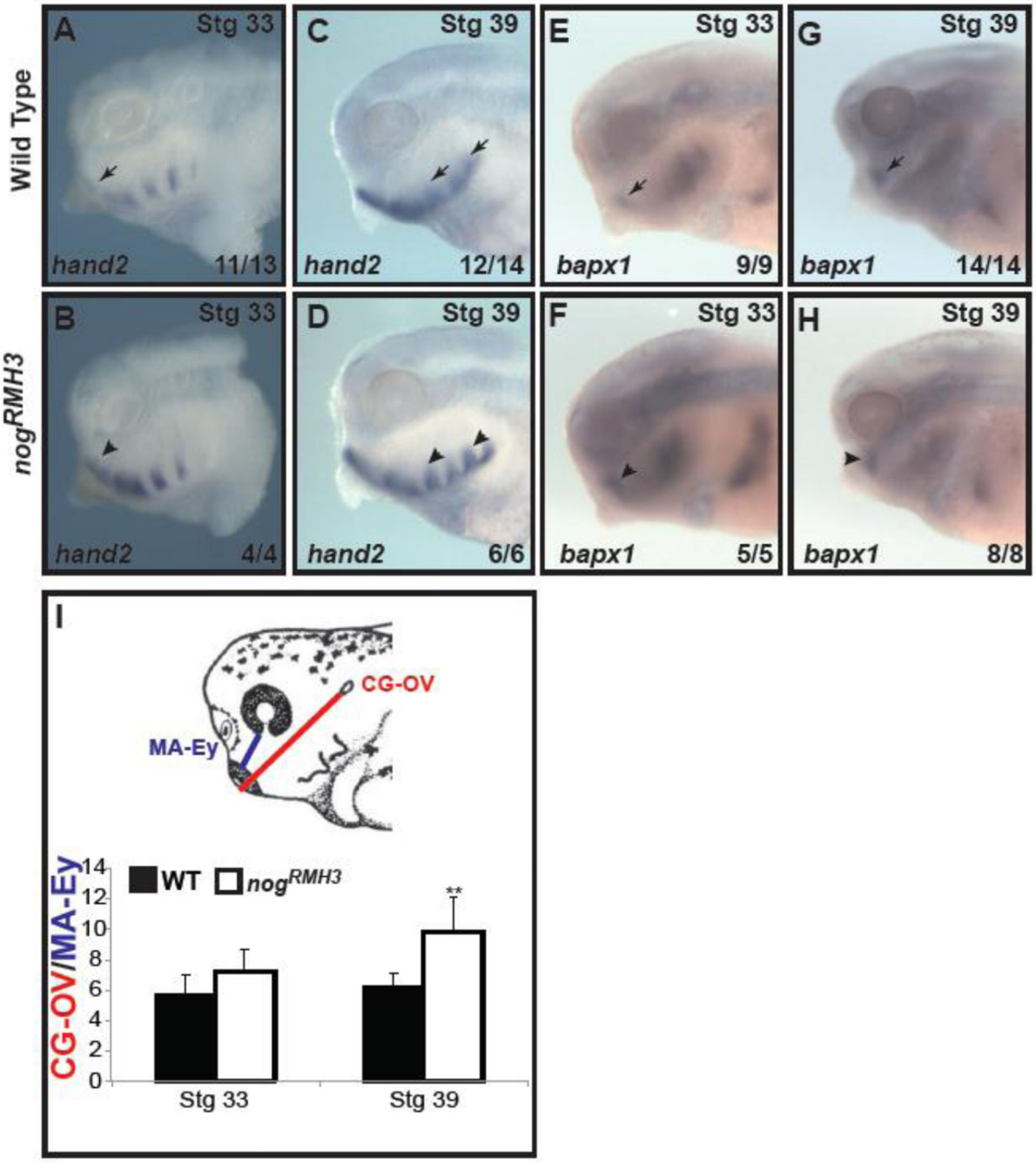

Figure 5. *hand2* and *bapx1* expression is altered in homozygous *nog*^{RMH3} mutant tadpoles

(A–D) Expression of *hand2* in the head of representative WT (A,C) and homozygous *nog*^{RMH3} (B,D) tadpoles. **(E–H)** Expression of *bapx1* in the head of representative WT (E,G) and homozygous *nog*^{RMH3} (F,H) tadpoles. (A–B,E–F) Stage 33. (C–D,G–H) Stage 39. Anterior to the left and dorsal towards the top. **(M)** Quantification of *bapx1* expression domain shift as measured by the cement gland (CG) to otic vesicle (OV) length divided by the stained mandibular arch (MA) to eye (Ey) length. Black bars indicate wildtype embryos and open bars show mutant embryos. ** indicates $p<0.05$ (T-test). (A,C,E,G) Arrows show

domains of expression of indicated genes in WT tadpoles. (B,D,F,H) Arrowheads show altered expression domains in homozygous *nog*^{RMH3} mutants.

Table 1

Frequency of observed mutants in matings of *Xenopus tropicalis* carrying the *nog*^{RMH3} allele.

Founder (Pair)	Total Tadpoles	Wild Type	Mutant
1	202	147 (72.7)	55 (27.3)
2	568	794 (76.7)	241 (23.3)
3	527	405 (76.9)	122 (23.1)
4	1612	1187 (73.6)	425 (26.4)
Totals	**3376**	**2533 (75.1)**	**843 (24.9)**